

Nuclear Structure of the even-even Argon isotopes with a focus on magnetic moments

S.J.Q. Robinson,¹ Y.Y. Sharon,² and L. Zamick²

¹ *Department of Physics, Millsaps College, Jackson, MS 39210,*

² *Department of Physics and Astronomy, Rutgers University, Piscataway NJ 08854*

(Dated: April 22, 2022)

We study the role of configuration mixing in the heavier even-even isotopes of Argon. We begin by limiting the configurations of the even-even Ar isotopes to $(d_{3/2}^2)_\pi (f_{7/2}^n)_\nu$. There, due to the particular location in this shell model space of ^{40}Ar and ^{44}Ar , we find that the spectra, $B(E2)$'s and magnetic moments of these two nuclei are identical. Any deviation from this equality is direct evidence of configuration mixing. In a larger shell model space there are significant differences between these two nuclei, with ^{44}Ar being more collective. We also consider other even-even isotopes of Argon and study how their nuclear structure effects evolve with N . We compare in the full $0\hbar\omega$ space $(sd)_\pi (fp)_\nu$ the results of calculations with the WBT interaction and with the newer SDPF, denoted SDPF-U, interaction.

PACS numbers:

I. INTRODUCTION

Previously members of our theoretical group were involved in collaborations with experimentalists from Rutgers and Bonn studying the properties of $^{36,38,40}\text{Ar}$ as well as $^{32,34,36}\text{S}$ [1, 2, 3, 4, 5, 6] with the focus being the magnetic dipole g factors of the 2_1^+ states. We also note the results for $^{38,40}\text{S}$ obtained in experiments carried out by Davies et al. and by Stuchbery et al. [7, 8].

In this work we accomplish two things. The first is that we observe that due to the half filled nature of the $d_{3/2}$ proton sub-shell in the results of calculations in the simplest single j shell picture, $(d_{3/2}^2)_\pi (f_{7/2}^n)_\nu$, for the even-even Argon isotopes beyond ^{36}Ar , certain symmetries emerge. These symmetries serve as a basis for comparison with large space calculations for which these symmetries no longer hold. Secondly, we extend the calculations of the properties of the even Ar nuclei to the more neutron rich Ar isotopes for which the 2_1^+ g factors have not yet been measured. These are $^{42,44,46}\text{Ar}$. In particular, we note interesting and important divergences in the results obtained with two different interactions in this region; the WBT interaction [9] and the updated SDPF interaction denoted SDPF-U [10, 11]. The shell model calculations using the WBT interaction were carried out with the OXBASH shell model code [12] and those using the SDPF-U interaction with the ANTOINE shell model code [13]. In all the calculations, the effective charges $e_p = 1.5$ and $e_n = 0.5$ were used as well as the free nucleon g factors.

We show in Table I, as a summary, the relevant previously obtained experimental and calculated g factors of 2_1^+ states, data which are contained in the work of Speidel et al. on ^{36}S [6]. There are several points of interest. For example, the g factors of the $N=Z$ nuclei ^{32}S and ^{36}Ar are purely isoscalar and are very close to 0.5, as was discussed before in papers with Speidel.

In ^{38}Ar we have a closed $d_{3/2}$ neutron shell in the above small space so the g factor is due to the $d_{3/2}$ protons. In this limit we have $g(2_1^+)^{38}\text{Ar} = g(\frac{3}{2}_1^+)^{39}\text{K}$. The measured values are $+0.24(12)$ and $+0.2610$, respectively. The error bars on ^{38}Ar are large but the results are thus far not inconsistent. The measured value for ^{39}K differs considerably from the bare value $g=+0.083$ for a $d_{3/2}$ proton.

TABLE I: Experimental and calculated $g(2_1^+)$ factors

	Z	N	experimental g factor	calculated g factor
Sulfur	Z=16	16	+0.45 (7)	+0.501
		18	+0.50(8)	+0.491
		20	+1.3(5)	+1.16
		22	+0.13(5) ^a	-0.055
		24	-0.01(6) ^a	+0.079
Argon	Z=18	18	+0.52 (18)	+0.488
		20	+0.24(12)	+0.309
		22	-0.02(2)	-0.195

a [7]

In [6] the comment was made that when one looks at the $g(2_1^+)$ data there is a shell break (at $N=20$) for the S isotopes but not for the Ar isotopes. However this can be easily understood.

For ^{36}S (with $N=20$) the basic configuration is a $s_{1/2}$ proton and a $d_{3/2}$ proton coupled to $J=2^+$. This is a stretched configuration with a g factor $0.5[\mu s_{(1/2)} + \mu d_{(3/2)}]$. The answer is dominated by the large $s_{1/2}$ magnetic moment. In the heavier S isotopes one puts neutrons into the $f_{7/2}$ shell, where their g factor is negative, and thus a big drop in $g(2_1^+)$ is expected and indeed is observed.

For ^{38}Ar (with $N=20$) the basic configuration is $d_{3/2}^2$ protons with a closed $s_{1/2}$ proton shell. This has a much smaller g factor than the $s_{1/2} d_{3/2}$ proton configuration. So when one goes to the heavier Ar isotopes by adding $f_{7/2}$ neutrons the drop is not so dramatic.

II. SMALL SPACE EQUALITIES

In order to see the evolution of configuration mixing we calculate the nuclear structure of several even-even isotopes of Argon in the small model space $(d_{3/2}^2)_\pi (f_{7/2}^n)_\nu$ with the WBT interaction with the A dependence removed. These results comprise a part of Tables II, III and IV.

The most striking feature of these results is that one gets identical results for many properties of ^{44}Ar and ^{40}Ar , including the spectra, $B(E2)$'s and g factors, as long as one uses the same interaction for all these nuclei.

Why the equality? It arises from the fact that the two $d_{3/2}$ protons are in mid-shell. In ^{40}Ar we have two valence $f_{7/2}$ neutrons while in ^{44}Ar we have two $f_{7/2}$ neutron holes. In general the particle-hole interaction is not the same as the particle-particle interaction. But the two $d_{3/2}$ protons are at mid-shell and so can also be regarded as two $d_{3/2}$ proton holes. The hole-hole interaction (up to a constant) is equal to the particle-particle interaction. This basically proves the relationship between ^{40}Ar and ^{44}Ar in the small space. As a beautiful consequence of this relationship, any divergence between these two nuclei in the $0\hbar\omega$ larger-space calculations, and more importantly, in experimental observations, is a direct result of configuration mixing.

III. EVOLUTION IN THE WBT CALCULATIONS FROM THE SMALL $(d_{3/2}^2)_\pi (f_{7/2}^n)_\nu$ SPACE TO THE LARGE $0\hbar\omega (sd)_\pi^2 (fp)_\nu^n$ SPACE

a. The 2_1^+ excitation energy in the small and large spaces

In Table II we show the experimental [22, 23] and calculated excitation energies in both the small and large spaces for the Ar isotopes using the WBT [9] interaction and the OXBASH [12] shell model code. We also include in that table the results of calculations in the larger space with the SPDF-U [10] [11] interaction using the ANTOINE shell model code [13].

In the present section we will compare the small space WBT results with the large space " $0\hbar\omega$ " results using the same interaction. By " $0\hbar\omega$ " we mean that the protons are restricted to the full s-d shell and the neutrons to the full f-p shell. In the next section, we will compare the WBT results with the results from the more recent SPDF-U interaction.

In the small space the calculated energies of the 2_1^+ states of $^{38,40,42,44,46}\text{Ar}$ are seen from Table II to be symmetric about ^{42}Ar . The big increase for ^{46}Ar is due to the fact that the eight $f_{7/2}$ neutrons form a closed shell. The excitation energy of the 2_1^+ state of ^{46}Ar (for a fixed A interaction) is the same as for ^{38}Ar .

However, the behavior in the large space is different. There is a steady decrease in the calculated excitation energy of the 2_1^+ state from 2.010 to 1.143 MeV as one goes from ^{38}Ar to ^{46}Ar . Overall there is fairly good agreement between the calculated large space results and the experimental values except for ^{46}Ar . (See Table II.)

We thus see a problem in understanding ^{46}Ar , one which we will address in a later section. The small space calculation yields a rise in the 2_1^+ energy of ^{46}Ar relative to ^{44}Ar , in agreement with experiment, but of too large a magnitude. There is no such rise in results of the large space calculations. On the other hand, the observed excitation energy in ^{38}Ar (2.167 MeV) is larger than the corresponding energy in ^{46}Ar (1.550 MeV) –in the small space they would be the same, at 2.118 MeV.

b. The g factors in the small and large spaces

The g factors for all the states of interest were calculated, using the free nucleon g factors, and are available in Table III. We focus on the $g(2_1^+)$ values. For the reasons previously noted, in the small space the $g(2_1^+)$ values for ^{40}Ar and ^{44}Ar are the same (-0.441). For ^{46}Ar in the small space, the $f_{7/2}$ neutron shell is filled, and its $g(2_1^+)$ factor

is the same ($g(2_1^+)=+0.083$) as that of ^{38}Ar (being due to the $d_{3/2}^2$ proton configuration). The other Ar isotopes have negative g factors in the small space calculations because of the contributions of the open-shell $f_{7/2}$ neutrons.

The above small space $g(2_1^+)$ numbers change considerably when the large space is considered. Note that for ^{38}Ar the change in the $g(2_1^+)$ values from the small space ($g(2_1^+)=+0.083$) to the large space ($g(2_1^+)=+0.308$) goes in the direction of the measured g factors for ^{38}Ar and ^{39}K , the former being $+0.24(12)$ [1] and the latter being $+0.26$ [24], indicating the importance of configuration mixing. In addition, in the large space there are further indications of substantial configuration mixing from the considerable differences in the $g(2_1^+)$ values between ^{38}Ar ($g(2_1^+)=+0.308$) and ^{46}Ar ($g(2_1^+)=+0.100$) and also between ^{40}Ar ($g(2_1^+)=0.197$) and ^{44}Ar ($g(2_1^+)=-0.022$). For the states of higher angular momentum, $J=4, 6$ and 8 , there is also a large amount of quenching of the g factors as one goes from the small space to the large space. For example for the unique configuration $J=8$ ($J_p=2, J_n=6$) in ^{40}Ar and ^{44}Ar , the g factor changes from -0.389 to -0.195 in ^{40}Ar and from -0.389 to -0.150 in ^{44}Ar . The measured value of $g(2_1^+)$ in ^{40}Ar is very small, $-0.02(2)$. This small value was explained in [2].

c. The B(E2) values in the small and large spaces

The experimental B(E2) values (taken from [23] and for ^{40}Ar from [5]), and the calculated B(E2) values in the small and large spaces, are given in Table IV.

In the small space both the $B(E2; 0_1^+ \rightarrow 2_1^+)$ and the $B(E2; 2_1^+ \rightarrow 4_1^+)$ each change by less than 16% as one moves from ^{38}Ar to ^{46}Ar . In the large space, however, these two calculated B(E2) values increase by respective factors of three and five, being largest for ^{46}Ar and ^{44}Ar respectively. The above large increase in the calculated values indicates that in the large space as one moves from ^{38}Ar to ^{46}Ar there is greater collectivity, as well as a reduction in the role played by the closure of the $f_{7/2}$ neutron shell at $N=28$, as configuration mixing effects become more important.

The experimental values for $B(E2; 0_1^+ \rightarrow 2_1^+)$ increase monotonically from ^{38}Ar to mid-shell, at ^{42}Ar , and then decrease until ^{46}Ar . The observed values are closer to the small space calculated values for ^{38}Ar and ^{46}Ar but closer to the large space values for $^{40,42,44}\text{Ar}$.

The very small value of the $B(E2; 0_1^+ \rightarrow 2_2^+)$ in ^{42}Ar in the small space is due to seniority considerations; this is discussed in Appendix A, where it is shown to be zero. In the $0 \hbar\omega$ calculations the values obtained for this B(E2) are 49.56 and $24 e^2 fm^4$ with the WBT and SDPF-U interactions, respectively. The experimental value from [14] is $19.5 e^2 fm^4$.

IV. COMPARISON OF $0\hbar\omega$ CALCULATIONS USING THE WBT AND SDPF-U INTERACTIONS

The SDPF interaction [11] is newer than the WBT interaction [9] and in addition its form was recently recast slightly to handle nuclei with $Z > 14$ differently than nuclei with $Z \leq 14$ [10]. This interaction is denoted by SDPF-U. The $Z > 14$ version of SDPF-U is the one used in this paper.

As much previous work has been carried out using the WBT interaction, it is valuable to compare the WBT results and conclusions to those which the SDPF-U interaction offers. The results for each nucleus are presented in Figures 1 thru 5, where the excitation energies are given in keV. The numerical results are simultaneously summarized for all five nuclei in Tables II, III, and IV. It is clear that, for the lower mass even-even Ar nuclei, the computed nuclear structure appears largely unchanged. In ^{44}Ar (Figure 4) some distinctions between the results with the two interactions begin to appear; in particular, the energies of the excited states above the 2_1^+ state are seen to diverge.

However, in ^{46}Ar (Figure 5) the two interactions now paint very different pictures of the low-energy nuclear structure of this nucleus. As was seen in [15, 16], the SDPF interaction, before its recent alterations, did very well in accounting for those energies of the levels of ^{46}Ar that could be firmly established. While the energies and g factors in ^{46}Ar are showing divergent behaviors between the WBT and SDPF-U interactions, we have nearly identical $B(E2; 0_1 \rightarrow 2_1)$ values in this nucleus for the two interactions, 541 in WBT and $525 e^2 fm^4$ in SDPF-U. However, these very similar calculated values for this B(E2) differ considerably from the experimental value of $196 e^2 fm^4$ reported in [17].

Indeed, in [17] the authors performed shell model calculations for several nuclei including ^{46}Ar . For that nucleus they also obtained much too large a B(E2) value. They used the Wildenthal interaction for the sd shell, the FPD6 interaction for the fp shell, and the cross-shell interaction of Warburton, Becker, Millener and Brown—see ref [17] for further details. On the other hand, they got good agreement for the energy of the 2_1^+ state. The fact that we here also obtain too large a B(E2) with yet two other different interactions indicates that this is a robust result. However, as noted again in [17], a different approach, the self-consistent mean-field calculations by Werner et al. [18], yields a much smaller B(E2) in close agreement with experiment. Using smaller effective charges will also reduce the calculated B(E2) values.

One main thrust of our work is to see the effects of the various shell model interactions on magnetic moments. Perhaps the most surprising result is that, although for most of the Ar isotopes the $g(2_1^+)$ values with the SDPF-U

are not so different from those of WBT, there is a very large difference for ^{46}Ar . There, whereas for WBT the value of $g(2_1^+)$ is 0.100, for SDPF-U it increases to +0.513. Likewise, the $g(2_2^+)$ values in ^{46}Ar are quite different, -0.070 and -0.514, respectively. Furthermore, for the $g(4_1^+)$ the corresponding values are -0.190 and -0.388, respectively. These large differences indicate the crucial importance of experiments to measure these g factors in ^{46}Ar in order to determine the efficacy of the otherwise excellent SDPF-U interaction.

In order to understand the above noted differences between the results of the two interactions, we look at selected configurations in ^{46}Ar in which the eight neutrons remain in the $f_{7/2}$ shell and close that shell. Three of these configurations are displayed in Table V. We then focus on the proton configurations, which are the only ones that matter in those cases. The g factor for the lowest single-particle energy configuration $d_{3/2}^2 s_{1/2}^2$ is small but the other two configurations have large positive g factors. What is most surprising is the very large occupation probability of the $d_{3/2}^3 s_{1/2}$ configuration (having a very large g factor, see Table V) in the 2_1^+ wavefunction with SDPF-U -21.77%. This occupation probability value is much larger than the corresponding result for the WBT interaction where it is only 2.51%. This goes a long way in explaining why the value of $g(2_1^+)$ in ^{46}Ar is larger for SDPF-U than for WBT.

To explain the large percentage occupancy of the $d_{3/2}^3 s_{1/2}$ configuration for SDPF-U, we show in Table VI the observed $J=\frac{3}{2}^+ - J=\frac{1}{2}^+$ splittings in the odd K isotopes. We see experimentally a steady reduction in this splitting as one goes from ^{39}K to ^{45}K and a crossover in ^{47}K , where $J=\frac{1}{2}^+$ becomes the ground state. In the calculated $J = \frac{3}{2}^+ - J = \frac{1}{2}^+$ splittings in Table VI, the WBT interaction gets some of the systematics correct, narrowing the gap as we approach ^{47}K and expanding it afterwards. However the SDPF-U is much better in this region, correctly giving the cross-over at ^{47}K and returning the states to the usual ordering at ^{49}K .

The idea, as pointed out in [10], is that the $0f_{7/2}$ neutron - $0d_{3/2}$ proton interaction is working to lower the $0d_{3/2}$ orbital. This makes the occupation of that orbital increasingly favorable as we fill the $0f_{7/2}$ orbit with neutrons. This effect is considerably more pronounced in the SDPF-U interaction than in the WBT interaction. In our case, we note in Table VII the increasing removal of protons from the $1s_{1/2}$ and their subsequent migration to the $0d_{3/2}$ as the neutron number increases from $N=20$ until $N=28$. If neutrons are added past $N=28$, the $1p_{3/2}$ neutrons behave in the opposite manner, working to make the $1s_{1/2}$ orbit lower. (We do wish to point out that work on the $J=\frac{3}{2}^+ - J=\frac{1}{2}^+$ splittings was carried out in more limited shell model spaces some time ago by Johnstone [19].)

There have also been discussions in the literature of the changes in the neutron single particle energies [20]. From the reaction $^{46}\text{Ar}(d,p)^{47}\text{Ar}$ these authors find reductions in both the f and the p single particle spin-orbit splittings in ^{47}Ar relative to its isotone ^{49}Ca . They attribute these changes to effects of the proton-neutron tensor interaction in the former case and to the density dependence of the spin-orbit interaction in the latter case.

It is interesting to calculate at $N=28$ the shell gap, i.e. the $p_{3/2}-f_{7/2}$ neutron single particle energy difference. This gap is given by the binding energy difference expression $\text{BE}(^{49}\text{Ca})+\text{BE}(^{47}\text{Ca}) - 2 \text{BE}(^{48}\text{Ca})$. With the SDPF-U interaction we calculate a value of 4.74 MeV for this gap. This value can be compared to the corresponding gap value from the experimental mass tables where we receive a value of 4.80 MeV in good agreement with the calculated value. We also note that these values are both larger than the splitting of the $J=\frac{3}{2}^- - J=\frac{1}{2}^-$ splitting in ^{41}Ca which is 1.9 MeV.

It should be emphasized that in the shell model calculations we perform it is not necessary to put in by hand the changes in single particle energies for different nuclei. A good effective interaction implicitly generates these changes, both for protons in the s - d shell and for neutrons in the f - p shell.

V. CONCLUSION

Several interesting results were pointed out in this study. The peculiar situation for ^{40}Ar and ^{44}Ar presents an excellent chance to experimentally examine configuration mixing, since any divergence in the experimentally measured properties of these two nuclei represents the effects of configuration mixing. In the naive shell model, they will have identical nuclear structure due to the half filling of the $d_{3/2}$ orbital. The results of allowing $0 \hbar\omega$ configuration mixing in the heavier isotopes of Argon is examined. As we increase in mass to ^{46}Ar we see a divergence in the results obtained with the widely-used WBT interaction and the newer SDPF-U interaction. The low energy near-yrast nuclear structure of ^{46}Ar that is obtained with these two interactions is presented and awaits more detailed experimental study.

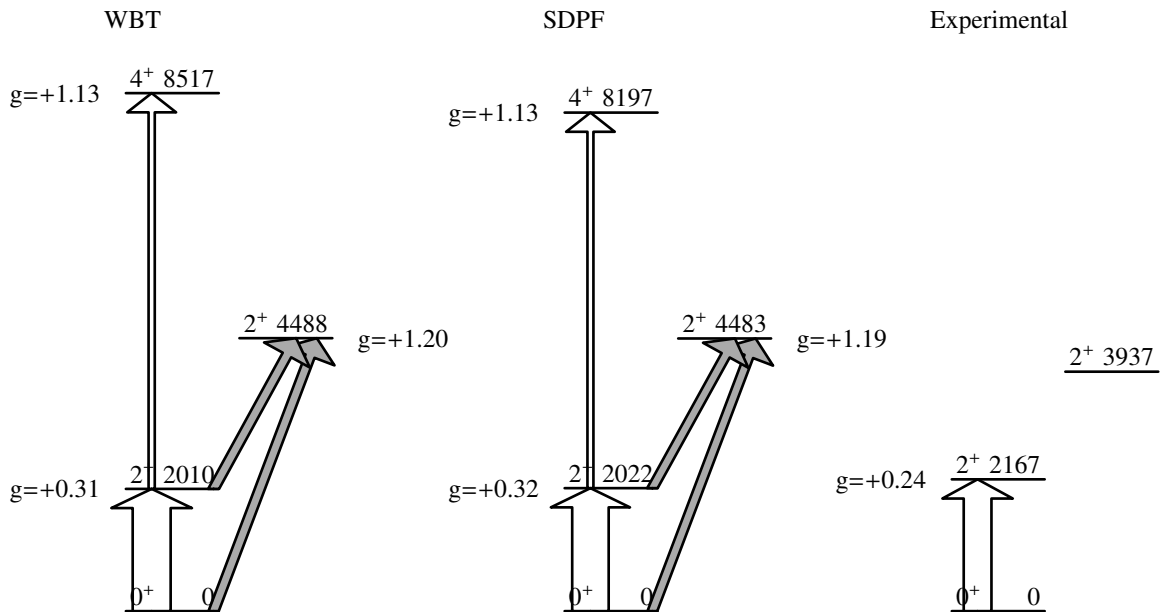


FIG. 1: ^{38}Ar , levels are labeled by excitation energy in keV and g factor. $B(E2 \text{ up})$ is proportional to width of the arrow.

VI. APPENDIX A

The vanishing of the $B(E2: 0_1^+ \rightarrow 2_2^+)$ in a small space calculation of ^{42}Ar can be explained by noting that both the proton and neutron configurations are at mid-shell $d_{3/2}^2 f_{7/2}^4$. The protons couple to J_p the neutrons couple to J_n , and J_p and J_n couple to J .

Here are all the configurations in the small space of $[J_p J_n]$ which lead to a total $J=0$ or total $J=2$.

$J=0$ $[0,0], [2,2], [2,2']$

$J=2$ $[0,2], [0,2'], [2,0], [2,2], [2,2'], [2,4], [2,4']$

In the above $J=2'$ and $J=4'$ designate seniority $v=4$ states of the $f_{7/2}^4$ neutron configuration. The states $J=2$ and $J=4$ have $v=2$ and $J=0$ has $v=0$.

Because we are at mid-shell the quantity $s = (-1)^{(v_p+v_n)/2}$ is a good quantum number. The wave functions have either $s=+1$ or $s=-1$.

For $J=0$

$s=1$ is a linear combination (lc) of $[0,0]$ and $[2,2]$

$s=-1$ $[2,2']$

For $J=2$

$s=-1$ is a lc of $[0,2], [2,0], [2,2'], [2,4']$

$s=1$ is a lc of $[0,2'], [2,2], [2,4]$

At mid-shell for particles of one kind there cannot be a $B(E2)$ between states of the same seniority (see e.g. Lawson [21]). We can use this to show that the $B(E2)$ from the state $J=2$ $s=1$ to $J=0$ $s=1$ must vanish.

For the $[2,2]$ to $[2,2]$ transition we can break things down so that we have a term with a transition from 2 to 2 for protons and a term with a transition from 2 to 2 for neutrons. In both cases we get a $v=2$ to $v=2$ transition which must vanish. The same story holds for the $[2,4]$ to $[2,2]$ transition. Consider next the $[0,2']$ term. It cannot connect to $[2,2]$. Less obvious is the connection of $[0,2']$ to $[0,0]$. This vanishes because the one body E2 operator cannot change the seniority by more than 2 units but here we require a change of four. (See eq. (A3.31) in Lawson [21]).

We have thus explained the vanishing $B(E2)$ in ^{42}Ar in the small space.

ACKNOWLEDGEMENTS:

The authors would like to thank Gulhan Gurdal, Noemie Koller, and Gerfried Kumbartski for their interest and

TABLE II: Excitation energies in MeV for the even-even Argon isotopes

Excitation energies	³⁸ Ar	⁴⁰ Ar	⁴² Ar	⁴⁴ Ar	⁴⁶ Ar
E(2₁⁺)					
experiment	2.167	1.464	1.208	1.144(17)	1.550(10)
small space WBT	2.118	1.254	1.272	1.254	2.118
0 $\hbar\omega$ WBT	2.010	1.424	1.292	1.172	1.143
0 $\hbar\omega$ SDPF-U	2.022	1.281	1.154	1.087	1.592
E(2₂⁺)					
experiment	3.937	2.524	2.487		
small space WBT	N/A	3.642	2.926	3.642	N/A
0 $\hbar\omega$ WBT	4.488	2.865	2.327	1.804	2.099
0 $\hbar\omega$ SDPF-U	4.483	2.911	2.276	1.775	3.772
E(4₁⁺)					
experiment		2.892			
small space WBT	N/A	2.750	2.422	2.751	N/A
0 $\hbar\omega$ WBT	8.517	2.742	2.430	2.719	2.759
0 $\hbar\omega$ SDPF-U	8.197	2.647	2.165	2.439	3.528
E(6₁⁺)					
experiment					
small space WBT	N/A	3.670	3.608	3.670	N/A
0 $\hbar\omega$ WBT	N/A	3.543	3.731	3.839	4.428
0 $\hbar\omega$ SDPF-U	N/A	3.204	3.323	3.174	5.322
E(8₁⁺)					
experiment					
small space WBT	N/A	6.703	5.846	6.703	N/A
0 $\hbar\omega$ WBT	N/A	6.573	5.821	6.199	6.638
0 $\hbar\omega$ SDPF-U	N/A	6.308	5.302	5.398	8.400

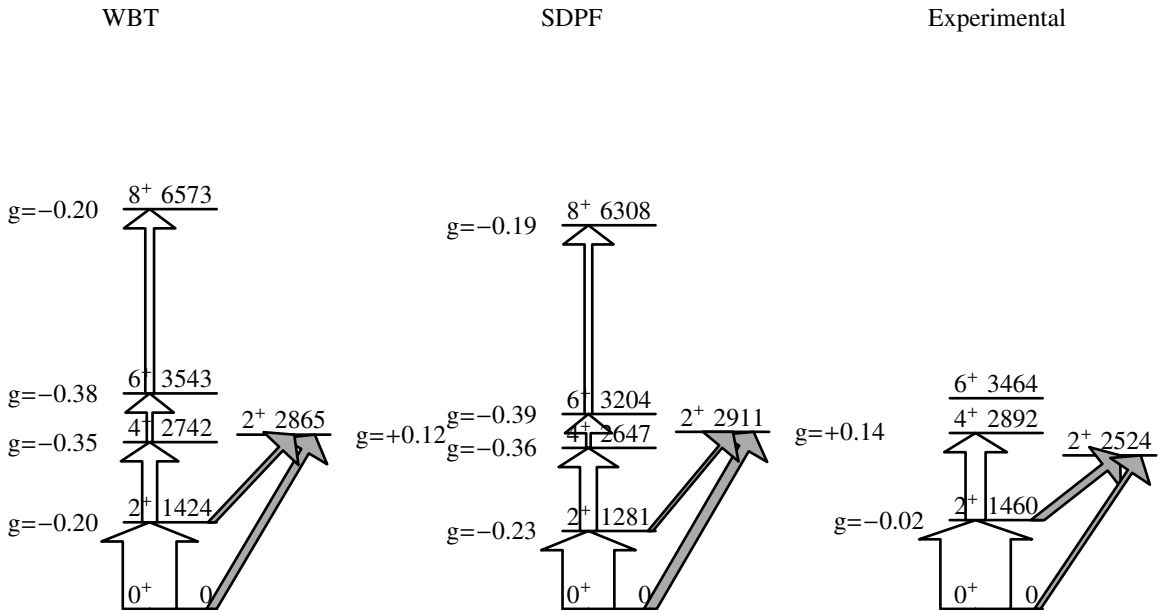
FIG. 2: ⁴⁰Ar, levels are labeled by excitation energy in keV and g factor. B(E2 up) is proportional to width of the arrow.

TABLE III: g factors in the even Argon isotopes
 g factors ^{38}Ar ^{40}Ar ^{42}Ar ^{44}Ar ^{46}Ar

$g(2_1^+)$						
experiment	0.24(12)	-0.02(2)				
small space WBT	0.083	-0.441	-0.455	-0.441	0.083	
$0 \hbar\omega$ WBT	0.308	-0.197	-0.095	-0.022	+0.100	
$0 \hbar\omega$ SDPF-U	0.319	-0.228	-0.084	-0.040	0.513	
$g(2_2^+)$						
experiment						
small space WBT	N/A	-0.046	-0.481	-0.046	N/A	
$0 \hbar\omega$ WBT	1.198	0.120	0.096	0.045	-0.070	
$0 \hbar\omega$ SDPF-U	1.187	0.136	0.075	0.346	-0.514	
$g(4_1^+)$						
experiment						
small space WBT	N/A	-0.490	-0.509	-0.490	N/A	
$0 \hbar\omega$ WBT	1.134	-0.354	-0.277	-0.206	-0.190	
$0 \hbar\omega$ SDPF-U	1.132	-0.357	-0.289	-0.246	-0.388	
$g(6_1^+)$						
experiment						
small space WBT	N/A	-0.525	-0.515	-0.525	N/A	
$0 \hbar\omega$ WBT	N/A	-0.381	-0.333	-0.313	-0.233	
$0 \hbar\omega$ SDPF-U	N/A	-0.394	-0.328	-0.301	-0.095	
$g(8_1^+)$						
experiment						
small space WBT	N/A	-0.389	-0.477	-0.389	N/A	
$0 \hbar\omega$ WBT	N/A	-0.195	-0.258	-0.150	-0.224	
$0 \hbar\omega$ SDPF-U	N/A	-0.188	-0.255	-0.084	-0.095	

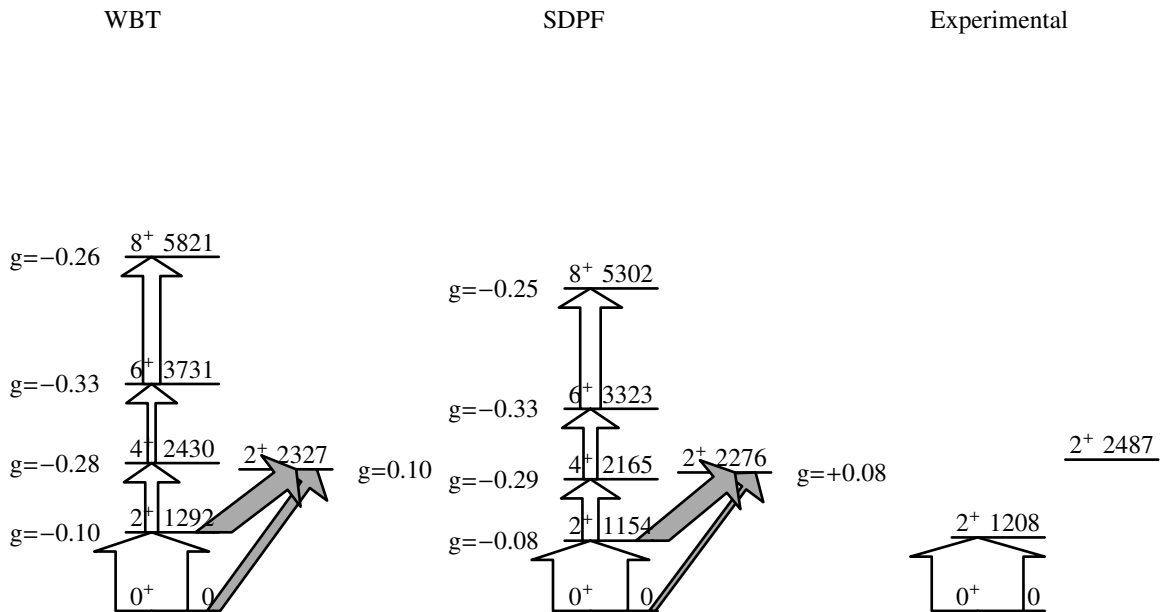


FIG. 3: ^{42}Ar , levels are labeled by excitation energy in keV and g factor. $B(E2 \text{ up})$ is proportional to width of the arrow.

TABLE IV: B(E2) values in $e^2 fm^4$ the even Argon isotopes

B(E2) values	³⁸ Ar	⁴⁰ Ar	⁴² Ar	⁴⁴ Ar	⁴⁶ Ar
B(E2; 0₁⁺ → 2₁⁺)					
experiment	130(10)	330(40)	430(100)	345(41)	196(39)
small space WBT	126.3	128.0	146.5	128.6	134.2
0 $\hbar\omega$ WBT	178.2	251.9	338.4	425.3	541
0 $\hbar\omega$ SDPF-U	171	243	351	357	525
B(E2; 0₁⁺ → 2₂⁺)					
experiment		24(4)	20 (9)		
small space WBT	N/A	51.71	0.000	52.05	N/A
0 $\hbar\omega$ WBT	45.48	41.3	49.56	57.82	2.081
0 $\hbar\omega$ SDPF-U	43	51.8	24	125	0.004
B(E2; 2₁⁺ → 2₂⁺)					
experiment		49(26)			
small space WBT	N/A	4.785	33.82	4.815	N/A
0 $\hbar\omega$ WBT	45.01	24.5	103.2	130.8	40.71
0 $\hbar\omega$ SDPF-U	43	17.79	98.3	125.5	0.221
B(E2; 2₁⁺ → 4₁⁺)					
experiment		94(14)			
small space WBT	N/A	48.10	52.46	48.38	N/A
0 $\hbar\omega$ WBT	28.97	70.14	59.64	157	143
0 $\hbar\omega$ SDPF-U	28	78.77	75	122.8	3.7
B(E2; 4₁⁺ → 6₁⁺)					
experiment					
small space WBT	N/A	18.18	38.86	18.26	N/A
0 $\hbar\omega$ WBT	N/A	27.25	37.02	61.56	112.6
0 $\hbar\omega$ SDPF-U	N/A	20.94	65	95.187	142.9
B(E2; 6₁⁺ → 8₁⁺)					
experiment					
small space WBT	N/A	33.33	44.65	33.50	N/A
0 $\hbar\omega$ WBT	N/A	40.87	80.99	122.8	82.91
0 $\hbar\omega$ SDPF-U	N/A	35.5	96	134	64.7

TABLE V: Percentage occupancy and g factors of configurations in the the 2₁⁺ wavefunction of ⁴⁶Ar in which the neutrons close the f_{7/2} shell.

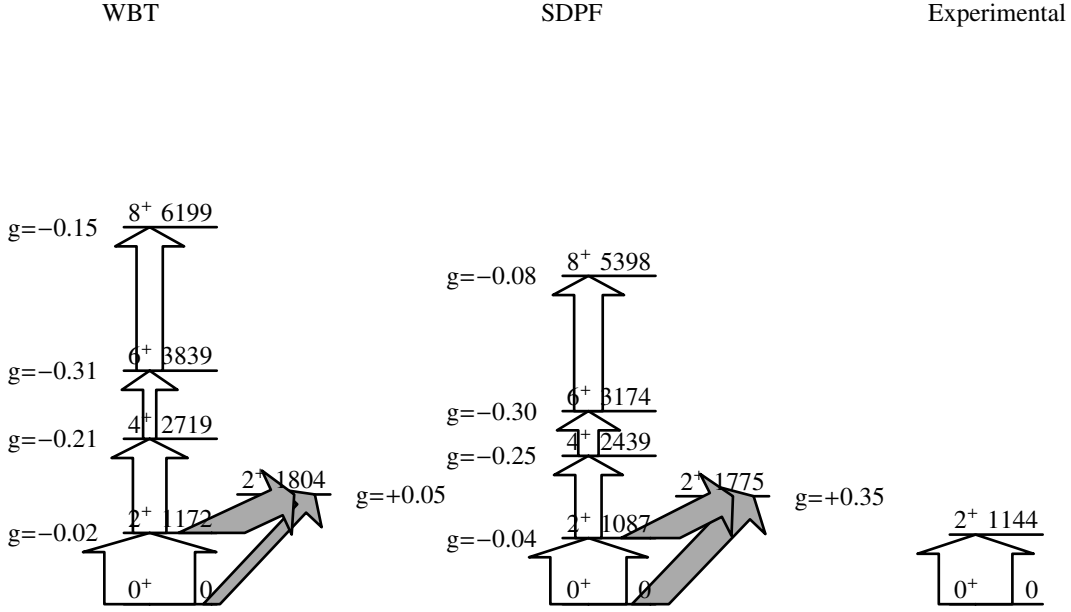
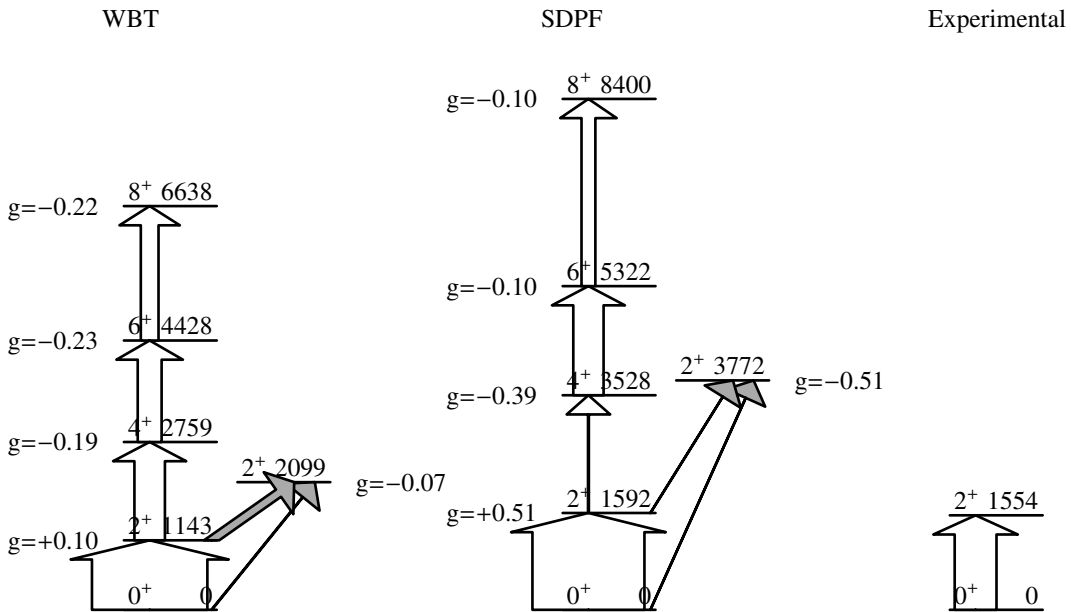
Proton configuration	Neutron configuration	SDPF-U	WBT	g factor
d _{3/2} ² s _{1/2} ²	f _{7/2} ⁸	1.08%	1.96%	+0.0828
d _{3/2} ³ s _{1/2}	f _{7/2} ⁸	21.77%	2.51%	+1.458
d _{5/2} ⁵ d _{3/2} ⁴ s _{1/2} ¹	f _{7/2} ⁸	3.60%	< 1.0%	+1.306

TABLE VI: The J=3/2⁺ - J=1/2⁺ splittings of the odd K isotopes in MeV.

	Experimental	WBT	SDPF-U
⁴¹ K	0.980476	1.106	0.854
⁴³ K	0.5612	1.109	0.672
⁴⁵ K	0.4745	0.871	0.345
⁴⁷ K	-0.3600	0.507	-0.320
⁴⁹ K	0.200	0.729	0.078

TABLE VII: The average proton occupation in the yrast 2^+ state of even Argon isotopes for the SDPF-U (WBT) interactions.

Neutrons	$1s_{1/2}$ average occupation	$0d_{3/2}$ average occupation
20	1.94 (1.94)	2.09 (2.085)
22	1.76 (1.84)	2.31 (2.22)
24	1.65 (1.80)	2.45 (2.29)
26	1.45 (1.73)	2.69 (2.38)
28	1.28 (1.66)	2.86 (2.45)

FIG. 4: ^{44}Ar , levels are labeled by excitation energy in keV and g factor. $B(E2 \text{ up})$ is proportional to width of the arrow.FIG. 5: ^{46}Ar , levels are labeled by excitation energy in keV and g factor. $B(E2 \text{ up})$ is proportional to width of the arrow.

encouragement.

- [1] K.-H Speidel et al., Phys. Lett. B **632**, 207 (2006).
- [2] E.A. Stefanova et al., Phys. Rev. C **72**, 014309 (2005).
- [3] S. Schielke et al., Phys. Lett. B **571**, 29 (2003).
- [4] K.-H Speidel et al., Phys. Rev. C **68**, 061302(R) (2003).
- [5] K.-H Speidel et al., Phys. Rev. C **78**, 017304 (2008).
- [6] K.-H. Speidel et al., Phys. Lett. B **659**, 101 (2008).
- [7] A.D. Davies et al., Phys. Rev. Lett. **96**, 112503 (2006).
- [8] A.E. Stuchbery et al., Phys. Rev. C **74**, 054307 (2006).
- [9] E. K. Warburton and B.A. Brown, Phys. Rev. C **46**, 923 (1992).
- [10] F. Nowacki and A. Poves, Phys. Rev. C **79**, 014310 (2009).
- [11] S. Nummela et al., Phys. Rev. C **63**, 044316 (2001).
- [12] A. Etchegoyen et al., computer code OXBASH, MSU-NSCL, Report No 524, 1985(unpublished).
- [13] E. Caurier and F. Nowacki, Acta Phys. Pol. B **30**, 705 (1999).
- [14] T.R. Fisher et al., Phys. Rev. C **9**, 598 (1974).
- [15] Zs. Dombradi et al., Nuc. Phys. A **727**, 195 (2003).
- [16] E. Caurier et al., Nuc. Phys. A **742**, 14 (2004).
- [17] H. Scheit et al., Phys. Rev. Lett. **77**, 3967 (1996).
- [18] T.R. Werner et al., Phys. Lett. B **335**, 259(1994); Nucl. Phys. A **597**, 327 (1996).
- [19] I.P. Johnstone, Phys. Rev. C **22**, 2561 (1980).
- [20] L. Gaudefroy et al., Phys. Rev. Lett. **97**, 092501 (2006).
- [21] R.D. Lawson, Theory of the Nuclear Shell Model, Clarendon Press Oxford, 1980.
- [22] ENSDF, <http://www.nndc.bnl.gov/nndc/ensdf/>.
- [23] S. Raman et al., At. Data Nucl. Data Tables **78**, 1 (2001).
- [24] N.J. Stone, At. Data Nucl. Data Tables **90**, 75 (2005).